Self-Assembly of Metal Nanoparticles and Nanotubes on Bioengineered Flagella Scaffolds

Mudalige Thilak Kumara,[‡] Brian C. Tripp,*[,†,‡] and Subra Muralidharan*[,‡]

Department of Biological Sciences, Mailstop 5410, Department of Chemistry, Mailstop 5413, and Nanotechnology Research and Computation Center, 1903 West Michigan Avenue, Western Michigan University, Kalamazoo, Michigan 49008

Received September 12, 2006. Revised Manuscript Received February 3, 2007

The previously described FliTrx *E. coli* flagellin protein was genetically engineered to display rationally designed histidine, arginine-lysine, and aspartic acid-glutamic acid peptide loops on the solvent-accessible outer domain region. The resulting flagellin monomers were self-assembled to obtain the corresponding oligomeric flagella bionanotubes in which the peptide loops were 5 nm apart. These flagella nanotubes were equilibrated with solutions of various metal ions (Co(II), Cu(II), Cd(II), Ag(I), Au(I), and Pd(II)). Controlled reduction of these metal ions yielded ordered arrays of nanoparticles or nanotubes, and in some cases, extensive aggregation resulted in formation of metal nanotube bundles. Both metal nanoparticles and nanotubes were generated with Cu(II) and Au(I), depending on the initial concentration of Cu(II) ions, while Ag(I) consistently formed metal nanowires, even under relatively mild conditions of reduction. The covalent attachment of separately synthesized Au nanoparticles to the flagella scaffold was also demonstrated. Controlled reduction of Co(II), Cd(II), and Pd(II) complexed with histidine and aspartic acid-glutamic acid peptide loops yielded ordered arrays of the respective metal nanoparticles on individual flagella nanotubes with minimal aggregation. The peptide loop modified flagella nanotubes have been demonstrated to be useful scaffolds for the generation of ordered arrays of metal nanoparticles or uniform nanotubes.

Introduction

The utilization of self-assembling biological systems in nanofabrication is attractive because of their genetically controlled reproducibility at the molecular level; they have the property of controlled self-assembly, often leading to the generation of less polydisperse nanoscale materials compared to chemical synthetic procedures. In addition, biomaterials are environmentally friendly and have a higher probability for biocompatibility. Peptide and protein assemblies are being actively investigated as nanotube templates for casting metal nanowires and nanotubes, and as scaffolds for the self-assembly of nanoparticles.[1,2] One example of a self-assembling protein nanotube is the M13 virus, which has been genetically engineered to display peptides on its surface.[3−5] These phage-displayed peptides may be selected for specific affinity for inorganic materials[6,7] and used as scaffolds for the controlled assembly or generation of inorganic nanoparticles and nanowires.[8−14] Furthermore, self-assembling beta-amyloid peptides, composed of a fragment of a Sup35p prion determinant from *Saccharomyces cerevisiae*, have also been demonstrated for the assembly of gold and silver nanowires.[15] Microtubules and peptide nanotubes have also been used as scaffolds for binding nanoparticles and as templates for the synthesis of monodisperse nanoparticles and metal nanotubes.[1,16−26] The resulting nanostructures prepared with

* Corresponding authors. B. Tripp: e-mail, brian.tripp@wmich.edu; fax, (269) 387-5609; phone, (269) 387-4166. S. Muralidharan: e-mail, subra.murali@wmich.edu; fax, (269) 387-2909; phone, (269) 387-3656.

[†] Department of Biological Sciences and Nanotechnology Research and Computation Center.

[‡] Department of Chemistry and Nanotechnology Research and Computation Center.

(1) Zhao, X.; Zhang, S. *Trends Biotechnol.* **2004**, *22* (9), 470−6.
(2) Wu, L. Q.; Payne, G. F. *Trends Biotechnol.* **2004**, *22* (11), 593−9.
(3) Sidhu, S. S. *Biomol. Eng.* **2001**, *18* (2), 57−63.
(4) Szardenings, M. *J. Recept. Signal Transduct. Res.* **2003**, *23* (4), 307−49.
(5) Kehoe, J. W.; Kay, B. K. *Chem. Rev.* **2005**, *105* (11), 4056−72.
(6) Whaley, S. R.; English, D. S.; Hu, E. L.; Barbara, P. F.; Belcher, A. M. *Nature* **2000**, *405* (6787), 665−8.
(7) Sanghvi, A. B.; Miller, K. P.; Belcher, A. M.; Schmidt, C. E. *Nat. Mater.* **2005**, *4* (6), 496−502.
(8) Lee, S. W.; Mao, C.; Flynn, C. E.; Belcher, A. M. *Science* **2002**, *296* (5569), 892−5.
(9) Mao, C.; Flynn, C. E.; Hayhurst, A.; Sweeney, R.; Qi, J.; Georgiou, G.; Iverson, B.; Belcher, A. M. *Proc. Natl. Acad. Sci. U.S.A.* **2003**, *100* (12), 6946−51.
(10) Nam, K. T.; Peelle, B. R.; Lee, S.-W.; Belcher, A. M. *Nano Lett.* **2003**, *4* (1), 23−7.
(11) Mao, C.; Solis, D. J.; Reiss, B. D.; Kottmann, S. T.; Sweeney, R. Y.; Hayhurst, A.; Georgiou, G.; Iverson, B.; Belcher, A. M. *Science* **2004**, *303* (5655), 213−7.
(12) Huang, Y.; Chiang, C. Y.; Lee, S. K.; Gao, Y.; Hu, E. L.; De Yoreo, J.; Belcher, A. M. *Nano Lett.* **2005**, *5* (7), 1429−34.
(13) Nam, K. T.; Kim, D. W.; Yoo, P. J.; Chiang, C. Y.; Meethong, N.; Hammond, P. T.; Chiang, Y. M.; Belcher, A. M. *Science* **2006**, *312* (5775), 885−8.
(14) Lee, S. K.; Yun, D. S.; Belcher, A. M. *Biomacromolecules* **2006**, *7* (1), 14−7.
(15) Scheibel, T.; Parthasarathy, R.; Sawicki, G.; Lin, X. M.; Jaeger, H.; Lindquist, S. L. *Proc. Natl. Acad. Sci. U.S.A.* **2003**, *100* (8), 4527−32.
(16) Matsui, H.; Pan, S.; Gologan, B.; Jonas, S. H. *J. Phys. Chem. B* **2000**, *104* (41), 9576−9579.
(17) Mertig, M.; Kirsch, R.; Pompe, W. *Appl. Phys. A* **1998**, *66*, S723−S727.
(18) Banerjee, I. A.; Yu, L.; Matsui, H. *Proc. Natl. Acad. Sci. U.S.A.* **2003**, *100* (25), 14678−82.
(19) Banerjee, I. A.; Yu, L.; Matsui, H. *J. Am. Chem. Soc.* **2003**, *125* (32), 9542−3.

10.1021/cm062178b CCC: $37.00
Published on Web 03/13/2007

these biomaterials and other organic and inorganic materials have been proposed to function as conducting wires for use in microcircuits, optical signal enhancing cuvettes, lithium ion batteries, and catalysts and as tool kits for the fabrication of nanoparticles.[1,2,8−14,16−63]

Bacterial flagella are another example of a natural, self-assembling protein nanotube. Flagella are elongated helical protein filaments, up to 10−15 μm in length, that are rotated to provide propulsion of bacterial cells.[64] Flagellar genetic components, protein structures, export and assembly processes, and biological functions are reviewed elsewhere[65−69] (see Supporting Information for a more detailed description of flagella). The flagellar filament is uniform in its dimensions, with a typical diameter of 12−25 nm, and consists of a helical assembly of the flagellin protein, with 11 protein subunits per turn.[70] Flagellin is a globular protein that is composed of four distinct domains: D0, D1, D2, and D3.[70] The D0, D1, and perhaps part of the D2 domains are essential for self-assembly into flagella fibers, while regions of the D2 domain and all of the D3 domain are highly variable,[71] dispensable,[72−75] and available for point mutation, deletion, and insertion of loop peptides, as previously demonstrated.[69,76−81] Thus, engineered flagella can function as bionanotube scaffolds of uniform diameter, with well-defined functional groups displayed on their surfaces,[82] and are ideally suited as scaffolds and templates for the generation of ordered arrays of nanoparticles and uniform, monodisperse nanotubes.[69,77]

The FliTrx flagellin peptide display system[79−81] contains a partial substitution of the D2 and D3 domains of *E. coli* flagellin (FliC) with the *E. coli* thioredoxin (TrxA) protein[83,84]

(20) Banerjee, I. A.; Yu, L.; Matsui, H. *J. Am. Chem. Soc.* **2005**, *127* (46), 16002−3.
(21) Matsui, H.; Gologan, B.; Pan, S.; Douberly, G. E., Jr. *Eur. Phys. J. D* **2001**, *16* (1−3), 403−6.
(22) Matsui, H.; Pan, S.; Douberlt, G. E. *J. Phys. Chem. B* **2001**, *105* (9), 1683−6.
(23) Djalali, R.; Chen, Y. F.; Matsui, H. *J. Am. Chem. Soc.* **2002**, *124* (46), 13660−1.
(24) Banerjee, I. A.; Yu, L.; Matsui, H. *Nano Lett.* **2003**, *3* (3), 283−7.
(25) Li, L.-S.; Stupp, S. I. *Angew. Chem., Int. Ed.* **2005**, *44* (12), 1833−6.
(26) Fu, X.; Wang, Y.; Huang, L.; Sha, Y.; Gui, L.; Lai, L.; Tang, Y. *Adv. Mater.* **2003**, *15* (11), 902−6.
(27) Richter, J.; Seidel, R.; Kirsch, R.; Mertig, M.; Pompe, W.; Plaschke, J.; Schackert, H. K. *Adv. Mater.* **2000**, *12* (7), 507−10.
(28) Storhoff, J. J.; Lazarides, A. A.; Mucic, R.; Mirkin, C.; Letsinger, R.; Schatz, G. C. *J. Am. Chem. Soc.* **2000**, *122* (19), 4640−50.
(29) Barbic, M.; Mock, J. J.; Smith, D. R.; Schultz, S. *J. Appl. Phys.* **2002**, *91* (11), 9341−5.
(30) Behrens, S.; Rahn, K.; Habicht, W.; Böhm, K.-J.; Rösner, H.; Dinjus, E.; Unger, E. *Adv. Mater.* **2002**, *14* (22), 1621−5.
(31) Harnack, O.; Ford, W. E.; Yasuda, A.; Wessels, J. M. *Nano Lett.* **2002**, *2* (9), 919−23.
(32) Hutter, E.; Fendler, J. H. *Chem. Commun.* **2002**, 378−9.
(33) Li, C. P.; Sun, X. H.; Wong, N. B.; Lee, C. S.; Lee, S. T.; Teo, B. K. *J. Phys. Chem. B* **2002**, *106* (28), 6980−4.
(34) Setlur, A. A.; Lauerhaas, J. M.; Dai, J. Y.; Chang, R. P. H. *Appl. Phys. Lett.* **1996**, *69* (3), 345−7.
(35) Dujardin, E.; Peet, C.; Stubbs, G.; Culver, J. N.; Mann, S. *Nano Lett.* **2003**, *3* (3), 413−7.
(36) Ellis, A. V.; Vijayamohanan, K.; Goswami, R.; Chakrapani, N.; Ramanathan, L. S.; Ajayan, P. M.; Ramanath, G. *Nano Lett.* **2003**, *3* (3), 279−82.
(37) Astruc, D.; Daniel, M. C.; Ruiz, J. *Chem. Commun.* **2004**, 2637−49.
(38) Song, Y.; Challa, S. R.; Medforth, C. J.; Qiu, Y.; Watt, R. K.; Peña, D.; Miller, J. E.; van Swol, F.; Shelnutt, J. A. *Chem. Commun.* **2004**, 1044−5.
(39) Ye, X.-R.; Lin, Y.; Wang, C.; Engelhard, M. H.; Wang, Y.; Wai, C. M. *J. Mater. Chem.* **2004**, *14*, 908−13.
(40) Sonnichsen, C.; Reinhard, B. M.; Liphardt, J.; Alivisatos, A. P. *Nat. Biotechnol.* **2005**, *23* (6), 741−5.
(41) Wang, Z.; Levy, R.; Fernig, D. G.; Brust, M. *Bioconjug. Chem.* **2005**, *16* (3), 497−500.
(42) Yu, S.; Welp, U.; Hua, L. Z.; Rydh, A.; Kwok, W. K.; Wang, H. H. *Chem. Mater.* **2005**, *17* (13), 3445−50.
(43) Sioss, J. A.; Keating, C. D. *Nano Lett.* **2005**, *5* (9), 1779−83.
(44) Hull, R. V.; Li, L.; Xing, Y.; Chusuei, C. C. *Chem. Mater.* **2006**, *18* (7), 1780−88.
(45) Ou, Y. Y.; Huang, M. H. *J. Phys. Chem. B* **2006**, *110* (5), 2031−6.
(46) Braun, E.; Eichen, Y.; Sivan, U.; Ben-Yoseph, G. *Nature* **1998**, *391* (6669), 775−8.
(47) Gao, P.; Zhan, C.; Liu, M. *Langmuir* **2006**, *22* (2), 775−9.
(48) Carny, O.; Shalev, D. E.; Gazit, E. *Nano Lett.* **2006**, *6* (8), 1594−7.
(49) Zheng, J.; Constantinou, P. E.; Micheel, C.; Alivisatos, A. P.; Kiehl, R. A.; Seeman, N. C. *Nano Lett.* **2006**, *6* (7), 1502−4.
(50) Radloff, C.; Vaia, R. A.; Brunton, J.; Bouwer, G. T.; Ward, V. K. *Nano Lett.* **2005**, *5* (6), 1187−91.
(51) Balmes, O.; Bovin, J. O.; Malm, J. O. *J. Nanosci. Nanotechnol.* **2006**, *6* (1), 130−4.
(52) Li, X.; Li, Y.; Yang, C.; Li, Y. *Langmuir* **2004**, *20* (9), 3734−9.
(53) Hassenkam, T.; Moth-Poulsen, K.; Stuhr-Hansen, N.; Norgaard, K.; Kabir, M. S.; Bjornholm, T. *Nano Lett.* **2004**, *4* (1), 19−22.
(54) Monson, C. F.; Woolley, A. T. *Nano Lett.* **2003**, *3* (3), 359−63.
(55) Lisiecki, I.; Filankembo, A.; Sack-Kongehl, H.; Weiss, K.; Pileni, M. P.; Urban, J. *Phys. Rev. B* **2000**, *61* (7), 4968.
(56) Jiang, X.; Herricks, T.; Xia, Y. *Nano Lett.* **2002**, *2* (12), 1333−8.
(57) Liu, Z.; Bando, Y. *Adv. Mater.* **2003**, *15* (4), 303−5.
(58) Gonzalez, J. C.; Rodrigues, V.; Bettini, J.; Rego, L. G. C.; Rocha, A. R.; Coura, P. Z.; Dantas, S. O.; Sato, F.; Galvao, D. S.; Ugarte, D. *Phys. Rev. Lett.* **2004**, *93* (12), 126103−4.
(59) Li, N.; Li, X.; Yin, X.; Wang, W.; Qiu, S. *Solid State Commun.* **2004**, *132* (12), 841−4.
(60) Luo, Y. H.; Huang, J.; Jin, J.; Peng, X.; Schmitt, W.; Ichinose, I. *Chem. Mater.* **2006**, *18* (7), 1795−1802.
(61) Ziegler, K. J.; Harrington, P. A.; Ryan, K. M.; Crowley, T.; Holmes, J. D.; Morris, M. A. *J. Phys. Condens. Matter* **2003**, *15* (49), 8303−14.
(62) Ren, L.; Guo, L.; Wark, M.; Hou, Y. *Appl. Phys. Lett.* **2005**, *87* (21), 212503−3.
(63) Bezemer, G. L.; Bitter, J. H.; Kuipers, H. P. C. E.; Oosterbeek, H.; Holewijn, J. E.; Xu, X.; Kapteijn, F.; vanDillen, A. J.; deJong, K. P. *J. Am. Chem. Soc.* **2006**, *128* (12), 3956−64.
(64) Bardy, S. L.; Ng, S. Y.; Jarrell, K. F. *Microbiology* **2003**, *149* (Pt 2), 295−304.
(65) Macnab, R. M. *Annu. Rev. Microbiol.* **2003**, *57*, 77−100.
(66) Macnab, R. M. *Biochim. Biophys. Acta* **2004**, *1694* (1−3), 207−17.
(67) Metlina, A. L. *Biochemistry (Moscow, Russ. Fed.)* **2004**, *69* (11), 1203−12.
(68) Malapaka, V. R.; Tripp, B. C. *J. Mol. Model. (Online)* **2006**, *12* (4), 481−93.
(69) Kumara, M. T.; Srividya, N.; Muralidharan, S.; Tripp, B. C. *Nano Lett.* **2006**, *6* (9), 2121−9.
(70) Yonekura, K.; Maki-Yonekura, S.; Namba, K. *Nature* **2003**, *424* (6949), 643−50.
(71) Beatson, S. A.; Minamino, T.; Pallen, M. J. *Trends Microbiol.* **2006**, *14* (4), 151−5.
(72) Kuwajima, G. *J. Bacteriol.* **1988**, *170* (7), 3305−9.
(73) Trachtenberg, S.; DeRosier, D. J. *J. Mol. Biol.* **1988**, *202* (4), 787−808.
(74) Mimori-Kiyosue, Y.; Yamashita, I.; Fujiyoshi, Y.; Yamaguchi, S.; Namba, K. *J. Mol. Biol.* **1998**, *284* (2), 521−30.
(75) Malapaka, R. R. V.; Adebayo, L. O.; Tripp, B. C. Generation and Characterization of Inorganic and Organic Nanotubes on Bioengineered Flagella of Mesophilic Bacteria. *J. Mol. Biol.* **2007**, *365* (44), 1102−16.
(76) Lu, Z.; Murray, K. S.; Van Cleave, V.; LaVallie, E. R.; Stahl, M. L.; McCoy, J. M. *Biotechnology (NY)* **1995**, *13* (4), 366−72.
(77) Kumara, M. T.; Muralidharan, S.; Tripp, B. C. *J. Nanosci. Nanotechnol.* **2007**, *7*, 1−13.
(78) Westerlund-Wikstrom, B. *Int. J. Med. Microbiol.* **2000**, *290* (3), 223−30.
(79) Lu, Z.; Murray, K. S.; Van Cleave, V.; LaVallie, E. R.; Stahl, M. L.; McCoy, J. M. *Biotechnology (NY)* **1995**, *13* (4), 366−72.
(80) Lu, Z.; Tripp, B. C.; McCoy, J. M. *Methods Mol. Biol.* **1998**, *87*, 265−80.
(81) Lu, Z.; LaVallie, E. R.; McCoy, J. M. *Methods Mol. Biol.* **2003**, *205*, 267−80.
(82) Fedorov, O. V.; Efimov, A. V. *Protein Eng.* **1990**, *3* (5), 411−3.
(83) LaVallie, E. R.; DiBlasio, E. A.; Kovacic, S.; Grant, K. L.; Schendel, P. F.; McCoy, J. M. *Biotechnology (NY)* **1993**, *11* (2), 187−93.
(84) LaVallie, E. R.; DiBlasio-Smith, E. A.; Collins-Racie, L. A.; Lu, Z.; McCoy, J. M. *Methods Mol. Biol.* **2003**, *205*, 119−40.

and can be used to express rationally designed amino acid sequences as constrained peptide loops on the surface of flagella. In this peptide display system, a multiple cloning site is present in the pFliTrx plasmid that corresponds to the solvent-exposed active site region of thioredoxin. As previously described,[69,77] 21 amino acid residues encoded in the multiple cloning site were removed by site-directed mutagenesis, and various DNA cassettes encoding constrained loop peptides of interest were inserted in this region. In one recent example, we demonstrated the engineering of flagellin proteins with 6 and 12 cysteine residues (with thiol side chains) displayed in the outer domain region, and the subsequent reversible self-assembly of their flagella nanotubes to form macroscopic bundles.[69] In another example, a 28-mer histidine loop (His loop) peptide composed of four repeats of an imidazole-rich Gly-His-His-His-His-His-His heptapeptide sequence (for a total of 24 histidine residues) was constructed.[69] These engineered FliTrx proteins were found to be efficiently expressed and exported into functional flagella fibers in *E. coli*. We have also successfully introduced other peptide loops, containing arginine and lysine, tyrosine and serine, or aspartic acid and glutamic acid residues, for the generation of various quantum dot nanoparticle arrays, and biomineral and organic polymer nanotubes.[77] Here, we describe the complementary exploration of this system for the generation of metal nanomaterials.

Gold nanoparticles and composite structures, e.g., nanowires, have been proposed to have applications as small capacitors, biosensors, and conductors.[12,16,21−26,28,31−33,35−37,40,41,45,49,50,53] The ordered assembly of gold nanoparticles is important because their optical properties depend on particle shape, size, the dielectric constant of the surrounding media, and the interparticle distance. Synthesis and assembly of gold nanoparticles and nanowires on carbon nanotubes,[36,45,85] silica nanotubes,[33] lipids,[51−53] virus particles,[12,35,50] DNA,[28,31,49] and self-assembling peptide nanotubes[16,21−26] have been described by several research groups. However, these methods may generate randomly distributed nanoparticles without consistent diameters and interparticle distances on the peptide or protein scaffolds.[31,49] Similarly, Cu nanotubes have been generated by vapor deposition, electrodeposition, and chemical methods[55−60] on carbon nanotubes,[34] by supercritical fluid decomposition on silica,[61] on DNA,[54] and on peptide nanotubes.[16,18] Studies have also been reported on the formation of Co nanoparticles and nanotubes on silica,[62] on carbon fibers for use as Fischer−Tropsch catalysts,[63] and on M13 virus particles.[13,14] Nanoparticles and nanotubes composed of the platinum group metals Pd and Pt have been synthesized by chemical methods,[42] in supercritical fluids,[39] on carbon nanotubes,[44] on DNA,[27] on protein and peptide nanotubes,[26,30,38] and on tobacco mosaic virus particles.[35] The generation of Ag nanoparticles and nanotubes has also been examined to a limited extent by chemical deposition methods on aluminum and polycarbonate membranes,[29,43] on DNA,[46] on peptide nanotubes,[47,48] and on tobacco mosaic virus particles.[35] Thus, biomolecules such as DNA, viruses, peptides, and proteins, as exemplified by these studies, are attractive and useful as scaffolds and templates for the generation of the nanoparticles and nanotubes of a variety of metals.

Flagella nanotubes are complementary to the various biological scaffolds that are being investigated for the generation of a uniform array of nanoparticles and nanotubes. Each segment of the flagella nanotube contains a flagellin protein 11-mer. Introduction of peptide loops in the D3 domain of the flagellin protein yields an extremely ordered array of binding sites for cations and anions which can be used as precursors for the generation of nanoparticles and nanotubes. Flagella nanotubes represent a system that can be manipulated for the generation of ordered nanomaterials for catalysis, molecular electronics, and other applications. In this study, FliTrx flagella engineered to display constrained peptide loops containing imidazole groups, cationic amine and guanido groups, and anionic carboxylic acid groups were used as scaffolds for the self-assembly of metal nanoparticles and nanotubes, as summarized in Table 1. The transition metal ion Co(II), the Group IB ions Cu(II), Ag(I), and Au(I), the Group IIB ion Cd(II), and the platinum group metal Pd(II) were complexed with histidine, arginine, lysine, aspartic acid, and glutamic acid residues in loop peptides and reduced with $NaBH_4$ or hydroquinone, in the case of Ag(I). These studies are complementary to other research efforts to exploit biological molecules as scaffolds and templates for the bottom-up construction of ordered nanomaterials.[8,11−14,16,18,19,22,23,25−27,30,35,38,46,47,50,54]

Experimental Section

Materials. The commonly employed chemicals and their sources and the instrumental techniques are listed here. More specific methods, chemicals, and instruments are described under appropriate sections. All chemicals were reagent grade or better and were obtained from Sigma-Aldrich (St. Louis, MO), unless otherwise noted. All transmission electron microscope (TEM) Formvar sample-imaging grids were obtained from Electron Microscopy Science (Fort Washington, PA). TEM images were taken with a JEOL model JEM 1230 TEM operating at 80 kV or a JEOL model 3011 TEM operating at 300 kV.

Engineering of FliTrx Flagella Loop Peptide Variants for Use as Bionanotube Scaffolds and Templates. The development of the FliTrx system for the display of constrained peptide loops on the surface of *E. coli* flagella fibers has been previously described.[62,63] As detailed in a previous publication,[69] the multiple cloning site region of the commercially available pFliTrx plasmid, which encoded a foreign peptide, was removed and replaced with the wild-type thioredoxin active-site DNA sequence, which encoded a unique RsrII restriction site. Furthermore, a non-native cysteine residue with a thiol side chain was mutated to serine to minimize the potential for intermolecular disulfide bond formation. The resulting modified pFliTrx plasmid is suitable for insertion of DNA oligonucleotide cassettes that encode displayed loop peptides in the solvent-exposed thioredoxin active site on the surface of FliTrx flagella.

The loop peptides chosen for this study were primarily composed of histidine, glutamic acid and aspartic acid, or arginine and lysine amino acid residues. Oligonucleotides encoding the loop peptides used in this study are described in the Supporting Information; the modified plasmid DNA was isolated and insertional mutations were confirmed by DNA sequencing (see Supporting Information). The

(85) Han, L.; Wu, W.; Kirk, F. L.; Luo, J.; Maye, M. M.; Kariuki, N. N.; Lin, Y.; Wang, C.; Zhong, C. J. *Langmuir* **2004**, *20* (14), 6019−25.

Table 1. Summary of Nanomaterials Prepared in This Study Using Engineered Flagella Nanotubes as Scaffolds

peptide loop type[a]	metal species	nanoparticle synthesis	resulting nanomaterial
histidine loop[b]	Au (gold)	synthesis of gold nanoparticles on flagella by reduction of Au(I) ions	linear flagella−Au nanotube bundles with discrete gold nanoparticles attached (Figure 1)
arginine-lysine loop[c]	Au (gold)	previously synthesized 3 and 10 nm gold nanoparticles covalently attached by amine coupling to arginine-lysine peptide loop flagella	aggregates of linear flagella−Au nanocomposite bundles (Figure 3)
histidine loop[b]	Cu (copper)	synthesis of discrete copper nanoparticles and continuous nanotubes on flagella by reduction of Cu(II) ions with $NaBH_4$	linear flagella−Cu nanotube bundles with discrete Cu nanoparticles and single linear Cu nanotubes (Figure 5)
a. aspartic acid-glutamic acid loop[d]	Co (cobalt)	synthesis of cobalt nanoparticles on flagella by reduction of Co(II) ions with $NaBH_4$	a. ordered array of Co nanoparticles on Asp-Glu loop flagella nanotubes (Figures 7a and 7b)
b. histidine loop[b]		note: cobalt oxides may be present on surface of nanoparticles	b. fractal-like dense assembly of flagella−Co to form nanoparticle composite on His loop flagella nanotubes (Figures 7c−7e)
histidine loop[b]	Pd (palladium)	synthesis of palladium nanoparticles on flagella by reduction of Pd(II) ions reduction with $NaBH_4$	single flagella−Pd nanoparticles; no extensive aggregation of the flagella (Figure 8)
histidine loop[b]	Cd (cadmium)	synthesis of cadmium nanoparticles on flagella by reduction of Cd(II) ions with $NaBH_4$	ordered array of nanoparticles on single and aggregated flagella nanotube fragments (Figure 9e)
aspartic acid-glutamic acid loop[d]	Ag (silver)	synthesis of silver and continuous silver nanowires on flagella by reduction of Ag(I) ions with hydroquinone	aggregated bundles and arrays of Ag−flagella nanowires (Figures 9a−9c)

[a] Type of genetically encoded, constrained loop peptide displayed on the surface of FliTrx flagella protein nanotubes. [b] Histidine loop peptide with 4 time repeat of the sequence: Gly-His−His-His−His-His−His (GHHHHHH), peptide has 24 histidine residues with imidazole groups. [c] Arginine-lysine loop peptide with a single insert of the sequence: Arg-Lys-Arg-Lys-Arg-Lys-Arg (RKRKRKR); peptide has 3 amine goups and 4 guanido groups. [d] Aspartic acid-glutamic acid loop peptide with 3 time repeat of the sequence: His-Asp-Glu-Asp-Glu-Asp-Glu (HDEDEDE); peptide has 3 imidazole and 18 carboxylate groups.

three loop peptides consisted of a 4 time insert of a one glycine, six histidine loop ("His loop") peptide containing imidazole groups (-Gly-His-His-His-His-His-His-; GHHHHHH), a 3 time insert of an anionic "Asp-Glu loop" peptide composed of one histidine residue, three aspartic acid residues, and three glutamic acid residues, and one glycine residue (-His-Asp-Glu-Asp-Glu-Asp-Glu-; HDEDEDE), and a single insert of a cationic "Arg-Lys loop" peptide encoding four arginine residues with guanido side chain groups and three lysine residues with amine side chain groups (-Arg-Lys-Arg-Lys-Arg-Lys-Arg-; RKRKRKR). Plasmids encoding the loop peptides were used to express FliTrx flagella fibers with peptide loops displayed on their surface and purified from *E. coli* (see Supporting Information).

Generation of Nanoparticle Arrays and Nanotubes on Flagella with Peptide Loops. In general, an appropriate metal ion or its complex was bound to the suitable peptide loop followed by controlled reduction to generate metal nanoparticle arrays and nanotubes on the flagella. Control experiments were performed with the wild-type (unmodified) flagella with all metal ions studied to demonstrate that they did not bind to the flagella and metal nanoparticles and nanotubes were not generated on the flagella when they were reduced, as indicated by TEM images. Examples of TEM images from control experiments have been included in the figures, demonstrating the generation of nanoparticles and nanotubes on flagella with peptide loops.

Generation of Gold Nanoparticle Arrays on Histidine Loop Flagella. Gold nanoparticles were synthesized using the His loop flagella as a nucleation template. Control experiments were also performed with the wild-type flagella to clearly indicate the role of the peptide loops in generating Au nanoparticle arrays on peptide-modified flagella. A volume of 500 μL of a 2 mg/mL solution of flagella with a 28-mer His loop peptide composed of four repeats of the Gly-His-His-His-His-His-His heptapeptide sequence (for a total of 24 histidines) was mixed with 10 μL of saturated chloro-(trimethylphosphine)gold(I) in deionized water at 4 °C. The Au complex was incubated with flagella for 24 h at 4 °C and reduced with 25 μL of 50 mM sodium borohydride solution at room temperature. TEM samples were prepared by placing 10 μL of the resulting solution on a carbon-coated Formvar copper grid for 2 min; excess solution was removed by blotting with a piece of filter paper.

Covalent Attachment of Gold Nanoparticles to Arginine-Lysine Loop Flagella. A different approach was used to covalently attach gold nanoparticles to an Arg-Lys loop flagella scaffold. Two sizes of 10-thioldecanoic acid-coated Au nanoparticles, 3 and 12 nm, were coupled to lysine amine groups in the Arg-Lys loop flagella. Synthesis of 3 and 12 nm diameter gold nanoparticles, protected by citrate, is described elsewhere.[32] The sizes of the nanoparticles were determined by TEM and showed a 10% polydispersity. The citrate coating on the Au nanoparticles was replaced with 10-thioldecanoic acid, and the carboxylic groups were further modified to sulfo-succinamide esters by reaction with 1-ethyl-3-(3-dimethylaminopropyl)-carbodiimide and sulfo-*N*-hydroxysuccinamide at pH 7 in 50 mM HEPES buffer. The resulting surface-modified Au nanoparticles were well-dispersed in water and the excess reactants were removed by diafiltration with a Centricon 3 kDa MWCO centrifugal filter unit (Millipore, Billerica, MA), using excess buffer. The Au nanoparticles, with amine-reactive surface groups, were dispersed in 100 μL of 20 mM HEPES buffer, and 10 μL of this suspension was mixed with 200 μL of 2 mg/mL of flagella with a single insert of the Arg-Lys loop peptide (RKRKRKR). After 30 min, 10 μL of this mixture was placed on a carbon-coated Formvar copper grid and allowed to settle on the grid for 1 min. Excess solution was removed by blotting with filter paper and TEM images were collected.

Generation of Copper Nanoparticle Arrays and Nanowires on Histidine Loop Flagella. Cu(II) ions in a 5 mM solution of $CuCl_2$, $CuSO_4$, or $Cu(NO_3)_2$ were allowed to complex with the imidazole side chains of the His loop flagellin histidine residues and wild-type flagella for control experiments for 24 h at 4 °C at

pH 7.0. Immobilized Cu(II) ions were reduced by successive addition of 20 μL of freshly prepared 100 mM $NaBH_4$ solution at 4 °C. The same procedure was followed to synthesize copper nanoparticles on the His loop flagella template using a 0.05 mM Cu(II) solution. The resulting Cu nanoparticle or Cu nanotube flagella composites were immobilized on a carbon-coated Formvar copper TEM grid by placing 10 μL of the resulting solution on the grid. After 1 min, excess solution was removed by blotting with filter paper and TEM images were recorded.

Generation of Cobalt Nanoparticles on Histidine Loop Flagella. These studies were extended to the transition metal Co, the Group IB metal Ag, the Group IIB metal Cd, and the platinum group metal Pd. In all cases, suitable divalent metal ions (Co(II), Cd(II), and Pd(II)) were complexed to imidazole groups on His loop flagella and wild-type flagella for control experiments and reduced in a controlled manner with $NaBH_4$. In the case of Ag(I) and Co(II) ions, complexation with Asp-Glu peptide loops and subsequent Ag(I) reduction with a hydroquinone solution at a pH of 10.5, and Co(II) reduction with $NaBH_4$, were also studied. The immobilization and subsequent reduction of Co(II), Cd(II), Pd(II), and Ag(I) ions had to be carried out on a TEM grid and immediately characterized. This was in contrast to the studies with Cu(II) and Au(I) described above, where the immobilization and reduction studies were conducted in bulk solution in vials, and nanotube samples were subsequently placed on carbon-coated Formvar copper TEM grids for image characterization.

Cobalt nanoparticles were generated by careful reduction of Co^{2+} ions complexed with histidine imidazole groups on the 4 time insert His loop FliTrx variant (with 24 histidine residues), or aspartic acid and glutamic acid carboxylic acid groups on the Asp-Glu loop flagella. The Asp-Glu variant used in this study had an insert of three repeats of the anionic Asp-Glu loop sequence (HDEDEDEG-HDEDEDEG-HDEDEDEG), for a total of 18 carboxylate groups and three histidine groups. Flagella with His loop or Asp-Glu loop peptides were immobilized on a carbon-coated Formvar copper TEM grid and 10 μL of 50 mM $CoCl_2$ solution was placed on the grid for 1 min. Excess solvent was removed by blotting with a piece of filter paper, followed by a 5 min reduction with 10 μL of 10 mM $NaBH_4$ solution and collection of TEM images.

Generation of Palladium and Cadmium Nanoparticles on Aspartic Acid-Glutamic Acid Loop Flagella. Palladium and cadmium nanoparticles were generated on His loop flagella using the same procedure used for cobalt. A 50 mM $CdCl_2$ solution and a saturated solution of palladium acetate, prepared by sonicating excess palladium acetate in deionized water followed by centrifugation to remove insoluble residues, were used as precursors for the formation of metal nanostructures.

Generation of Silver Nanowires on Aspartic Acid-Glutamic Acid Loop Flagella. Silver nanowires were generated by immobilizing Ag(I) on anionic Asp-Glu loop flagella and wild-type flagella (control) deposited on a carbon-coated Formvar copper grid and careful reduction with $NaBH_4$. A 10 μL volume of 20 mM $AgNO_3$ solution (pH adjusted to 10.5 with ammonium hydroxide) was placed on the TEM grid with immobilized flagella for 1 min and excess solution was removed by blotting with filter paper. Immobilized silver ions were reduced with 10 μL of 10 mM hydroquinone solution (pH adjusted to 10.5 with ammonium hydroxide) for 5 min and TEM images were collected.

Results and Discussion

The various types of FliTrx loop-nanomaterial systems used in this study are summarized in Table 1, including the FliTrx peptide loop composition, the use of pre-synthesized nanoparticles vs templated synthesis in situ, and the resulting type of hybrid nanomaterial, i.e., nanoparticle arrays or continuous nanotubes.

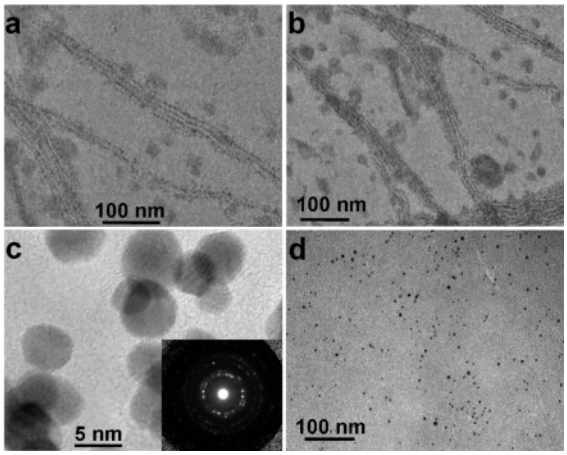

Figure 1. Gold nanoparticle−flagella nanotube composite materials obtained by reduction of Au(I). (a) and (b) TEM images of gold nanoparticles that were synthesized by reduction of Au(I) on a histidine loop peptide flagella scaffold. (c) High-resolution TEM image of individual gold nanoparticles on flagella; (inset) electron diffraction pattern of gold nanoparticles on flagella, indicative of metallic gold nanoparticles. (d) TEM image of control experiment of the reduction of Au(I) on wild-type (without histidine loops) flagella, indicating no attachment of Au and only random distribution of Au nanoparticles.

1. Generation of Gold Nanoparticle Arrays on Histidine Loop Flagella. This procedure yielded 5.93 (±1.48) nm diameter Au nanoparticles attached to the surface of the flagella scaffold as determined by TEM. Representative TEM images are shown in Figure 1, where images (a) and (b) were taken with flagella on a carbon-coated Formvar copper grid, image (c) is a high-resolution image of gold nanoparticles, and image (d) is the result of Au nanoparticle generation on wild-type flagella. The Au nanoparticles define the outer edge of the flagella nanotubes as they are bound to the solvent-exposed D3 domain. The Au nanoparticles are not bound to the wild-type flagella which lack the histidine loops as evident from Figure 1d. The process of Au nanoparticle formation is proposed to first involve binding of Au(I) ions by imidazole groups of the solvent-exposed loop peptide histidine residues, followed by reduction of Au(I) ions to Au(0) by controlled addition of $NaBH_4$. These histidine-bound Au(0) centers serve as nucleating sites for the growth of Au nanoparticles by the reduction of unbound Au(I). In the absence of histidine loops with wild-type flagella free Au nanoparticles are formed in solution as seen in Figure 1d.

The visible absorption spectrum of the 6 nm Au nanoparticles on the His loop flagella scaffold is shown in Figure 2a. The Au−flagellin nanocomposite exhibited an absorption maximum (λ_{max}) at 522.5 nm due to surface plasmon resonance of the Au nanoparticles. The TEM image of the flagella indicated an ordered array of Au nanoparticles on the flagella backbone. The Au nanoparticles are presumably bound to the histidine peptide loops on the flagellin D2−D3 outer domain region. The longitudinal axial distance between two consecutive D3 domains of flagella is approximately 5 nm.[70] Thus, the ordered arrangement of the Au nanoparticles is probably a direct result of the ordered

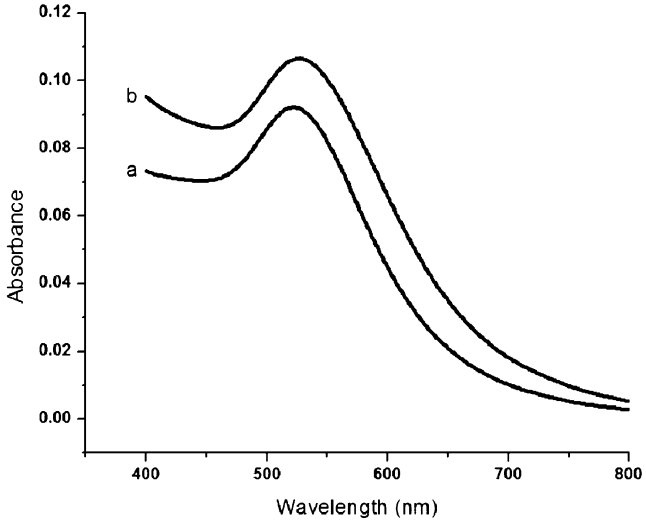

Figure 2. Visible absorbance spectra of gold nanoparticles on histidine loop peptide flagella. (a) Absorbance spectrum of gold nanoparticles synthesized on flagella, showing surface plasmon resonance peak. (b) Absorbance spectrum of gold nanoparticle−flagella sample after heating to 80 °C for 5 min and cooling to room temperature.

display of the peptide loops at regular intervals on the flagella scaffold surface. Some lateral association of flagella with Au nanoparticles occurred, as observed in Figures 1a and 1b, where bundled assemblies of two and three flagella fibers can be seen. However, the aggregation was not so extensive as to adversely affect the surface plasmon resonance, as shown in Figure 2a.

The effect of disassembly of the flagella scaffold on the Au nanoparticle surface plasmon resonance was also investigated. The aggregated flagella nanotubes with bound Au nanoparticles were dissociated by heating them to 80 °C for 5 min and cooling to 25 °C. The mesophilic FliTrx *E. coli* flagella oligomers will dissociate into flagellin protein monomers over the temperature range of 50−60 °C. The heated and cooled Au−flagellin solution exhibited a 16% increase in absorbance intensity and a ∼5 nm shift in λ_{max} to 527 nm (Figure 2b). The heating and cooling process, in addition to breaking up multimeric nanotube assemblies, also resulted in the formation of monomeric flagella and free gold nanoparticles as discerned from TEM images; dissociated Au nanoparticles precipitated from this heated solution within 2 h. Thus, the absorbance increase was likely due to disassembly of the flagella aggregates and dissociation of Au nanoparticles from the flagella nanotubes, with the small red shift in λ_{max} due to aggregation of disassembled nanoparticles.

2. Covalent Attachment of Gold Nanoparticles to Arginine-Lysine Loop Flagella. Covalent attachment of the pre-synthesized 3 nm Au nanoparticles by a published method[31] resulted in the formation of ca. 500 nm diameter flagella bundles with a dense layer of Au nanoparticles, as indicated in Figures 3a and 3b. A high-resolution TEM image of individual Au nanoparticles is shown in Figure 3c. A schematic diagram depicting the covalent amide bond formed between the terminal amine groups of lysine residues and the outer carboxylate groups of the surface-modified Au nanoparticles is shown in Figure 4. Amide bond formation between Au nanoparticles and flagella Arg-Lys loop peptides

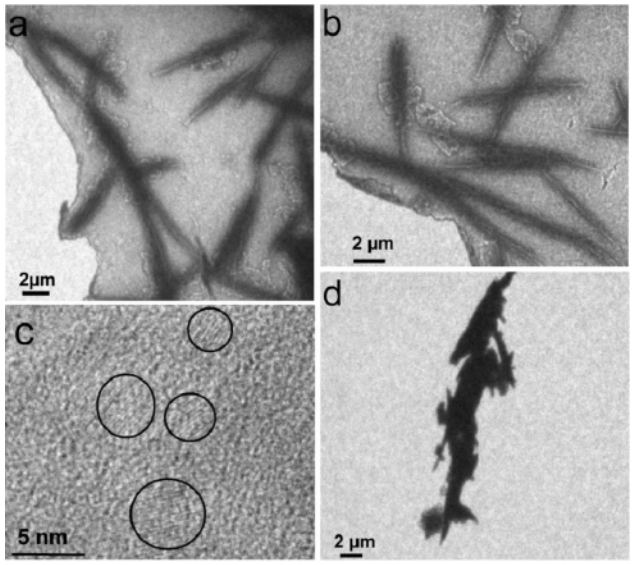

Figure 3. Gold nanoparticle−flagellin nanotube composite materials prepared by covalent attachment of pre-made gold nanoparticles. (a) and (b) TEM images of 3 nm gold nanoparticles attached by amine coupling to arginine-lysine peptide loop flagella. (c) High-resolution TEM image of 3 nm gold nanoparticles attached to flagella. (d) TEM image of 10 nm gold nanoparticles attached by amine coupling to arginine-lysine peptide loop flagella. These images are representative of the aggregated bundles generated by this procedure.

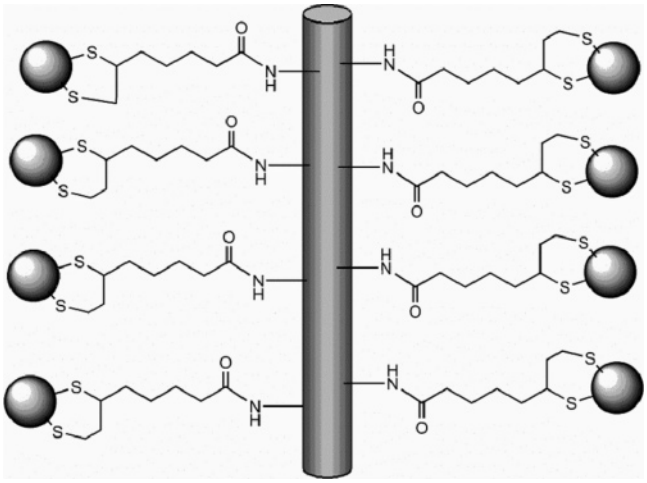

Figure 4. Diagram of covalent immobilization of pre-made gold nanoparticles on flagella by amide bond formation with arginine-lysine peptide loops.

resulted in extensive aggregation of flagella due to the multiple attachment sites available on both the derivatized nanoparticles and flagella with Arg-Lys loops. In contrast, binding of $Au(P(CH_3))_3Cl$ on histidine imidazole groups of His loop flagella and controlled synthesis by reduction with $NaBH_4$ resulted in generation of ordered arrays of Au nanoparticles and limited aggregation of flagella nanotubes. Covalent attachment of the larger 12 nm Au nanoparticles to the Arg-Lys loop flagella resulted in formation of larger, more extensive aggregates (Figure 3d) than were observed for the 3 nm Au nanoparticles; these larger Au-flagellin aggregates were not stable in solution and rapidly precipitated.

3. Generation of Copper Nanoparticle Arrays and Nanowires on Histidine Loop Flagella. Both individual Cu nanoparticles (Figure 5d) and continuous Cu nanotubes

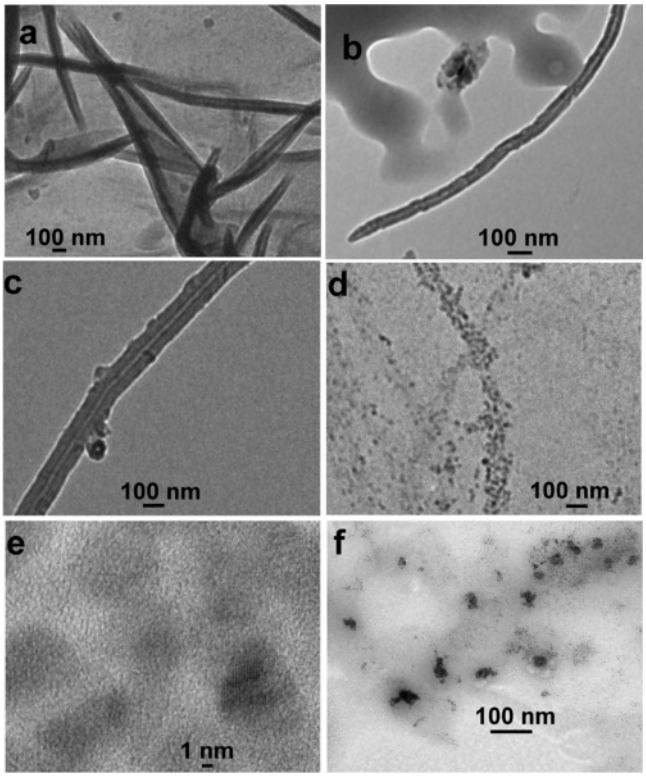

Figure 5. Copper−flagellin composite nanomaterials. (a), (b), and (c) TEM images of copper nanotubes synthesized by reduction of Cu(II) on histidine loop flagella. (d) TEM image of copper nanoparticles synthesized by reduction of Cu(II) on histidine loop flagella. (e) High-resolution TEM image of copper nanoparticles synthesized on histidine loop flagella. (f) TEM image of control experiment of the reduction of Cu(II) on wild-type (without histidine loops) flagella, indicating no attachment of Cu and only random distribution of Cu nanoparticles and clusters.

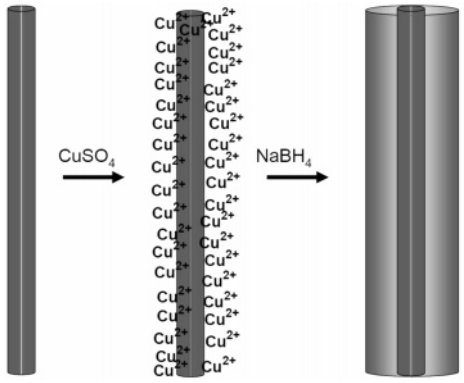

Figure 6. Proposed mechanism of copper nanoparticle (2) and nanotube (3) formation on histidine loop peptide flagella (1) scaffold by binding and reduction of Cu(II) ions.

(Figures 5a−5c) could be generated on the flagella backbone when Cu(II) ions were complexed with imidazole in the His loop peptide and reduced with 10 mM $NaBH_4$ in a controlled manner. A schematic of the probable mechanism of formation of Cu nanoparticles and nanotubes is given in Figure 6. The Cu nanotubes were generated by the reduction of 5 mM Cu(II) with 100 mM $NaBH_4$ and their TEM images are shown in Figures 5a−5c. It is evident from these images that the flagella nanotube has facilitated the formation of Cu nanotubes by the growth of a layer of Cu on the flagella. Most of the Cu nanotubes had a diameter of approximately 100 nm. The uniformity of growth of Cu nanotubes on the flagella templates is striking compared to that of Au, which resulted in formation of dense bundles. TEM images of flagella with Cu nanoparticles are shown in Figure 5d, with a corresponding high-resolution TEM image of the Cu nanoparticles shown in Figure 5e. The flagella fibers prepared with Cu nanoparticles did not exhibit much aggregation, unlike those with Au nanoparticles. Clearly, the behavior of the two Group IB metals, Cu and Au, is quite different under the experimental conditions studied. This may be the consequence of the oxide layer formation on Cu to a greater extent compared to Au which inhibits aggregation. Only free Cu nanoparticles were obtained as seen in Figure 5f when wild-type flagella were employed, clearly indicating the role of the histidine loop peptides in facilitating the formation of Cu nanotubes and ordered array of Cu nanoparticles.

The formation of Cu nanoparticles and nanotubes can be rationalized by the reduction of Cu(II) complexed with histidine to form nucleating sites, on which further growth of Cu metal occurs from free Cu(II) ions in solution. When a low concentration (0.05 mM) of Cu(II) was employed, the nucleation process resulted in formation of individual nanoparticles on the flagella scaffold. When a 100 times higher concentration (5.0 mM) of Cu(II) was employed, the nucleation process proceeded further, forming a continuous layer of Cu metal. The thin layer of Cu initially formed becomes the substrate for further growth of additional layers of Cu, leading to the generation of ∼100 nm diameter Cu nanotubes encasing the flagella nanotube templates. Experiments are underway to remove the flagella in a controlled manner to obtain pure Cu nanotubes. Such nanotubes can be further derivatized, e.g., via thiol chemistry, to attach various functional groups. Cu nanotubes functionalized with appropriate functional groups could function as a sensor platform and have applications in molecular electronics.

4. Generation of Cobalt Nanoparticles on Histidine Loop Flagella. Figures 7a and b indicate Co nanoparticles synthesized on Asp-Glu loop peptide flagella; Figures 7c−7e indicate Co nanoparticles synthesized on His loop flagella. Figure 7f indicates that the Co nanoparticles generated with the wild-type flagella leads to a mixture of the two instead of an array of nanoparticles on flagella when peptide loops are present. An ordered array of Co nanoparticles was obtained by reduction of Co(II) on Asp-Glu loop flagella (Figures 7a and 7b), while use of the His loop flagella scaffold resulted in formation of a more dense assembly of nanoparticles on the flagella (Figures 7c−7e). This result may be due to the higher affinity of the imidazole side chain of histidine for Co(II) transition metal ions, compared to the carboxylic side chains of glutamate and aspartate. The reduction of Co(II) was performed under ambient atmosphere; this suggests that the nanoparticle surfaces are most likely oxidized, resulting in formation of CoO, Co_2O_3, and Co_3O_4 oxide layers. Further studies are underway to characterize the nature of these nanoparticles by magnetic susceptibility measurements. We are also investigating their catalytic applications for reactions such as the Fischer−Tropsch alkane synthesis.[63]

5. Generation of Palladium and Cadmium Nanoparticles on Aspartic Acid-Glutamic Acid Loop Flagella. Figures 8a−8c indicate Pd nanoparticles synthesized on His

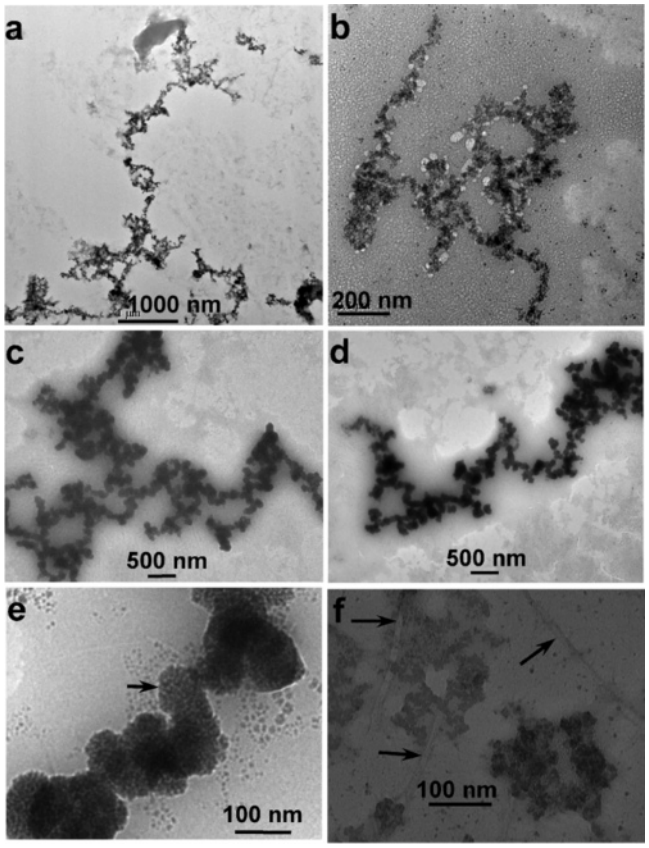

Figure 7. Cobalt−flagella composite nanomaterials. (a) and (b) TEM images of cobalt nanoparticles synthesized by reduction of Co(II) on glutamic acid-aspartic acid peptide loop flagella. (c), (d), and (e) TEM images of cobalt nanoparticles synthesized by reduction of Co(II) on histidine loop flagella. Arrow indicates Co nanoparticles. (f) TEM image of control experiment of the reduction of Co(II) on wild-type (without histidine loops) flagella, indicating no attachment of Co and only random distribution of Co nanoparticles and clusters and flagella nanotubes. Arrows indicate the presence separately of Co nanoparticles and flagella.

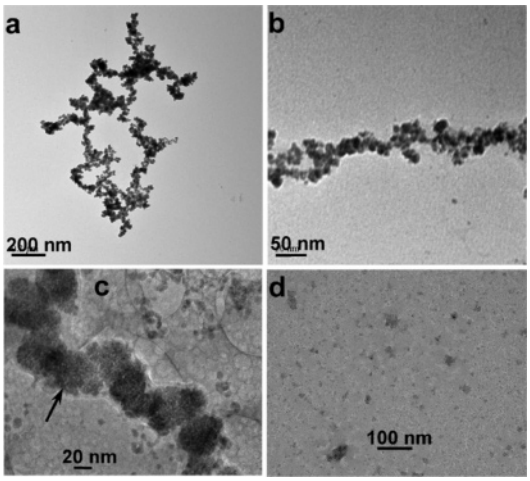

Figure 8. Palladium−flagellin nanocomposites. (a), (b), and (c) TEM images of palladium nanoparticles synthesized by reduction of Pd(II) on histidine loop flagella. Arrow indicates the Pd nanoparticles. (d) TEM image of control experiment of the reduction of Pd(II) on wild-type (without histidine loops) flagella, indicating no attachment of Pd and only random distribution of Pd nanoparticles.

loop flagella and Figure 8d the generation of Pd nanoparticles with the wild-type flagella. Figure 9e indicates Cd nanoparticles synthesized on His loop flagella and Figure 9f the generation of Cd nanoparticles in the presence of wild-type flagella. The controlled reduction with $NaBH_4$ of Pd(II) and

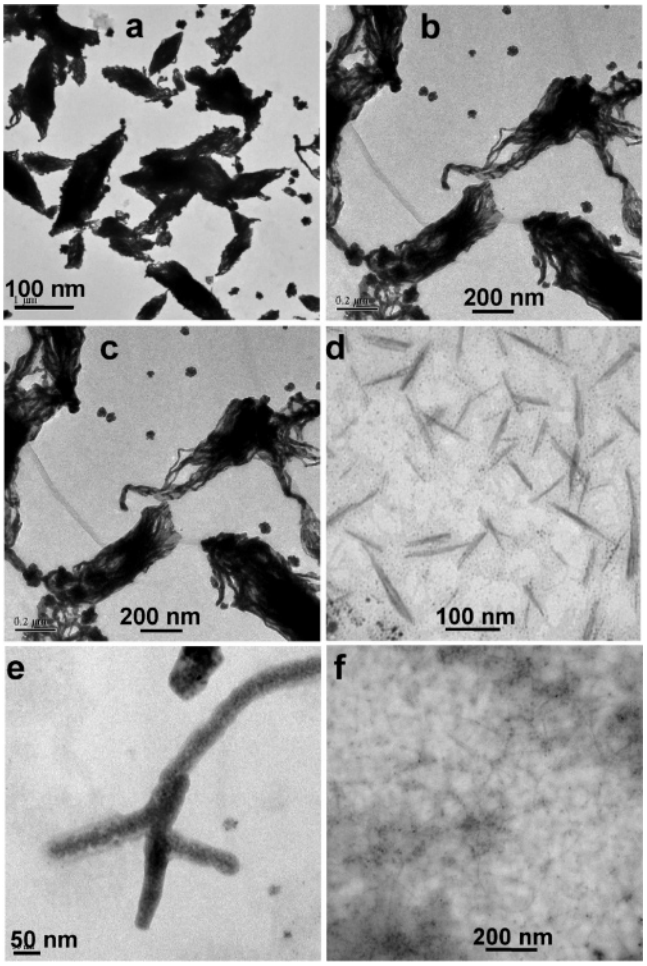

Figure 9. Silver−flagellin and cadmium−flagellin nanocomposite materials. (a), (b), and (c) TEM images of silver nanowires synthesized on flagella with glutamic acid-aspartic acid loop peptides. (d) TEM image of control experiment of the reduction of Ag(I) on wild-type (without histidine loops) flagella, indicating a weak association of Ag nanoparticles. (e) TEM image of cadmium nanoparticles synthesized on histidine loop flagella. (f) TEM image of control experiment of the reduction of Cd(II) on wild-type (without histidine loops) flagella, indicating no attachment of Cd and only random distribution of Cd nanoparticles and clusters.

Cd(II) complexed with the His loop flagella largely yielded nanoparticle arrays which were absent with the wild-type flagella. It may be seen from Figure 8c that Pd nanoparticles are present on the His loop flagella. The images in Figures 8a and 8b indicate that the formation of Pd nanoparticles did not result in extensive aggregation of the flagella. Some fragmentation of nanotubes resulting in a random distribution on the TEM grids was observed. Similarly, the formation of Cd nanoparticles on the His loop peptide flagella (Figure 9e) resulted in generation of an ordered array of nanoparticles and some fragmentation of the flagella and aggregation of fragments. Only random Cd nanoparticles could be detected with the wild-type flagella as seen in Figure 9f.

6. Generation of Silver Nanowires on Aspartic Acid-Glutamic Acid Loop Flagella. The reduction of Ag(I) complexed to aspartic acid-glutamic acid peptide loops was performed with hydroquinone instead of $NaBH_4$ to gain better control of the generation of nanoparticles. However, even this controlled mild reduction resulted in the formation of silver metal-covered flagella that were aggregated into bundles, as shown in Figures 9a−9c. The Ag wire structures

are evident in Figures 9a and 9b; Figure 9c indicates heavily aggregated nanowires leading to clumps of nanomaterials. Upon formation, the Ag nanoparticles rapidly seed the growth of further layers of Ag, analogous to our observations with higher concentrations of Cu(II). As a result, individual nanoparticles cannot be discerned, and instead, arrays of nanowires resulting from the rapid growth of Ag films on the flagella were observed. Further studies with various peptide loops are underway to determine conditions that will allow the more controlled formation of Ag nanoparticles on flagella. The ease of reduction of Ag(I) compared to Cu(II) results in the observed differences in reduction after they have been bound to peptide-modified flagella. This may account for the fact that, in the case of Ag as shown in Figure 9d, some deposition of these nanoparticles occurs even on the wild-type flagella. In general, it is useful to identify conditions under which nanoparticle arrays and nanowires can be formed, as the former are highly suitable for catalytic applications and the latter are more suitable for molecular electronics.

Conclusions

In summary, we have successfully demonstrated bioengineering of the FliTrx flagellin protein to generate flagella bionanotubes with high affinities for metal ions. A unique aspect of flagella is the ability to introduce peptide loops on monomers separated by 5 nm, with a high efficiency of loop peptide incorporation, resulting in evenly spaced binding sites, which make them attractive scaffolds for the generation of ordered arrays of nanoparticles and uniform nanotubes. Six different types of metal ions were complexed with the peptide loops and carefully reduced with $NaBH_4$ or hydroquinone to obtain metal−flagellin nanocomposites. The covalent attachment of previously synthesized Au nanoparticles to the flagella scaffold was also demonstrated. In most cases, the reductive chemistry procedures resulted in generation of ordered nanoparticle arrays on the flagellin bionanotube templates, although continuous metal nanowires were also generated with Ag(I) and higher concentrations of Cu(II). These nanowires could be electrically conductive and have applications in microelectronics. They could also be further derivatized through thiol chemistry to construct sensor arrays. The resulting flagella−Au nanoparticle arrays could have sensor applications, while the flagella−Co, Co_3O_4, and Pd nanoparticle arrays could have potential as chemical catalysts, with uniform particle sizes and high surface area to volume ratios. In general, nanoparticles, prisms, and rods would be useful for catalysis and sensor applications and nanowires for molecular electronics. These results, along with our previously reported studies on cysteine loop flagella and apatite, silica, and titania nanotube formation on flagella and polymerization of aniline bound flagella to form polyaniline bundles,[1,2] are a complementary set of investigations aimed at demonstrating the efficacy of bioengineered flagella as scaffolds and substrates for the generation of novel bionanomaterials with many potentially useful applications. These studies are also complementary to other similar studies reported in the literature employing peptide nanotubes, proteins, DNA, and viral capsids.[1,2,6−14,16−28,30,31,35,38,46−50,54]

Acknowledgment. This research was supported by the W. M. Keck Foundation and the Western Michigan University Nanotechnology Research and Computation Center.

Supporting Information Available: A detailed text description of bacterial flagella, procedures for flagellin mutagenesis, protein expression and purification and DNA sequences and translated protein sequences of thioredoxin active-site loop regions of the three FliTrx loop variants are given. This material is available free of charge via the Internet at http://pubs.acs.org.

CM062178B